Multihadron Production in Hadronic, Leptonic and Nuclear Reactions at High Energies*

Kisei KINOSHITA

Physics Department, Faculty of Education,

Kagoshima University, Kagoshima 890, Japan

Contents

---

*Lectures delivered at the KEK Summer School, August, 1979, and at the Department of Physics, Nagoya University, November, 1979.

1. Introduction

A universal aspect of multiparticle final states in high energy hadron- and lepton-induced reactions is the presence of jets of hadrons. A jet comes out along the direction of an incident hadron, or the direction of hardly scattered or produced constituent by some short distance interaction. Here, a jet is tentatively defined as a group of hadrons collimated along specific direction with limited transverse momentum spread characterized by finite $\langle p_T \rangle$ such as 0.4 GeV, and with scaled longitudinal distribution as a function of $z \sim p_\parallel / P_\parallel$ with respect to the parent momentum of the jet.

Such properties of jets, first established concerning forward and backward jets in soft hadron collisions (Fig. 1a), were also found in quark jets in the e^+e^- annihilation (Fig. 1b) and deep inelastic lepton-hadron scattering (Fig. 1c).[1] Although a quark does not come out as an isolated particle, the observation of the quark jet can be taken as the way of looking at it, as the bubbles in the bubble chamber exhibits the track of charged particles. Large p_T jets in hard hadron collisions (Fig. 1d), also show similar properties as the quark jets.[2]

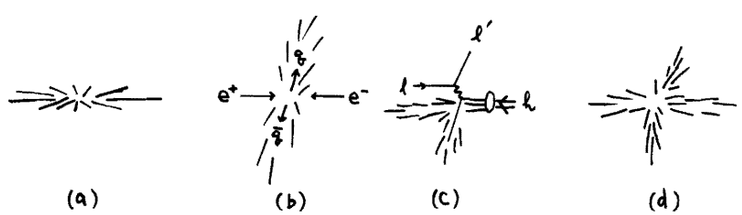

Fig. 1. Schematic illustration of jets in C.M.S.

In these lectures, I review theoretical attempts to understand the dynamics of jet formation, i.e., the mechanism of hadronization of hardly deflected (or created) constituent, and the dynamics of the fragmentation of an incident hadron into multihadron states owing to collision interaction. Since the relation between constituents and hadrons is most clearly seen in the distribution along the jet axis, I will concentrate on the problem of longitudinal distribution and discuss the underlying mechanism of how the total jet momentum is devided among produced hadrons.

It is now widely recognized that high energy phenomena should be understood on the basis of constituent dynamics and internal structure of hadrons. As for hard interaction at short time and distance, quantum chromo-dynamics (QCD)[3] is receiving increasing supports concerning various phenomenological consequences of its perturbative aspects.[4] A remarkable consequence of QCD is the existence of gluon jets, which are now showing up in the hadronic decay of the upsilon[5] and the three-jet structure of final states in the e^+e^- annihilation.[6] Furthermore, QCD revised the conventional picture of jets with limited $\langle p_T \rangle$ and scaled z distribution based on, now so called, naive parton model [7]. According to perturbative QCD approach, $\langle p_T \rangle$ of the quark (or gluon) jet increases almost linearly with the hardness Q of the short distance interaction, accompanied with mild scaling violation of the z distribution.[8] It is to be reminded, however, that the prediction of the QCD jet picture can be tested only for the data with wide range in Q, while the conventional jet picture works quite well as the first approximation.

On the other hand, the jet along an incident hadron, as well as

the soft hadronization process of the quark or gluon jet, cannot be dealt with by perturbative QCD method, since they are essentially non-perturbative phenomena and inevitably related to the confinement problem not yet solved. Therefore, at the present status, it is quite important to develop dynamical models based on composite structure of hadrons in order to attack the above problems. Along this direction, various models have been proposed and partly tested; some of them are models of quark-cascade,[9~11] quark-chain,[12~14] parton-recombination,[15,16] dressed quark fragmentation[17,18] and so on. In these lectures I will try to give a critical survey of these models and discuss their interrelations in order to attain integrated understanding of the jet dynamics.

The contents are organized as follows. We begin with the uncorrelated jet and parton models in Sect. 2 in order to clarify the implication of the kinematical constraint for the scaling. Sections 3, 5~7 are devoted to the survey of dynamical models. A brief introduction of the QCD jet picture is given in Sect. 4. Problem of the space-time evolution of hadronization process and comparison with nucleus target data are discussed in Sects. 8 and 9. Concluding remarks are given in Sect. 10.

2. Roots of $(1-x)^n$ behavior — Uncorrelated jet and parton models

Before going into specific dynamical assumptions, let us begin with kinematics of longitudinal phase space. It will be shown that the $(1-x)^n$ behavior ($x \sim 2p_{\parallel}/\sqrt{s}$), valid in various cases,[19] can be most simply obtained in the uncorrelated jet model[20], owing to

the kinematical constraint. The variation of n according to particle species requires more details about dynamics, as we discuss later.

Let us consider hadronic final states with two jet structure in the C.M.S. in the reaction

$$a + b \to \text{hadrons} ,$$

where a and b are the beam and target hadrons in the case of soft hadron collisions (Fig. 1a), or quark and antiquark in $e^+e^- \to q\bar{q} \to$ hadrons (Fig. 1b). We take the longitudinal axis along the momentum of a in the C.M.S., which is defined event by event in the e^+e^- annihilation, different from the e^+e^- axis. For simplicity, we disregard the p_T distribution and treat p_T as a constant.

We define light-like momenta $p_\pm$, rapidity y and transverse mass m_T of a produced hadron as

$$p_\pm \equiv E \pm p_{\parallel} = m_T e^{\pm y} ,$$
$$m_T = \sqrt{m^2 + p_T^2} , \tag{1}$$

where $p_\mu = (E, p_T , p_{\parallel})$ is the four-momentum of the hadron. In the following, we regard m_T as a small constant ($\lesssim$1 GeV), since we do not go into the p_T distribution.

Light-like fractions $x_\pm$ are defined by

$$x_\pm = \frac{E \pm p_{\parallel}}{\sqrt{s}} , \tag{2}$$

referring to the total energy $\sqrt{s}$ in the C.M.S.

At high enough energies, $x_\pm$ can be identified with the Feynman's longitudinal variable as

$$x_{\parallel} \equiv \frac{2p_{\parallel}}{\sqrt{s}} \sim x_+ \quad \text{at } x_{\parallel}>0, \quad \text{where } x_-\sim 0,$$
$$\sim -x_- \quad \text{at } x_{\parallel}<0, \quad \text{where } x_+\sim 0. \tag{3}$$

It often happens that light-like fractions become more convenient than $x_{\parallel}$, since they can be written as

$$x_+ = (E+p_{\parallel}) \,/\, (E+p_{\parallel})_a \ ,$$
$$x_- = (E-p_{\parallel}) \,/\, (E-p_{\parallel})_b \ . \tag{4}$$

which are invariant under longitudinal boost.

Energy momentum conservation constraint in the C.M.S. can be written as

$$\delta(\sqrt{s} - \Sigma_i E_i)\,\delta(\Sigma_i p_{i\parallel}) = \frac{2}{s}\delta(1-\Sigma_i x_{i+})\,\delta(1-\Sigma_i x_{i-})$$

The longitudinal phase space $dp_{\parallel}/E$, consisting of Lorentz invariant phase space $d^3p/E=dp_T dp_{\parallel}/E$, can be written as

$$\frac{dp_{\parallel}}{E} = dy = \frac{dx_+}{x_+} = -\frac{dx_-}{x_-} \ , \tag{5}$$

We drop dp_T in the following discussions, for simplicity.

2.1. Independence and democracy in longitudinal phase space

As a model of multiparticle final state with least dynamical assumptions except for the p_T cut off, we first consider uncorrelated jet model. For simplicity, we consider only one kind of particles with common m_T. Under the assumption of independent emission with strength λ, the exclusive n-particle distribution is given by

$$p_n(y_1,y_2\cdots y_n) \equiv \frac{1}{\sigma_{tot}} \frac{d\sigma_n}{dy_1\cdots dy_n}$$
$$= N_0 \frac{\lambda^n}{n!}\,\delta(1-\Sigma_i x_{i+})\,\delta(1-\Sigma_i x_{i-}) \ , \tag{6}$$

where N_0 is an overall normalization, and $\sigma_{tot} = \Sigma_n \sigma_n$. In this model, produced particles are completely democratic in the longitudinal phase space.

Since $x_+x_- = m_T^2/s \sim 0$, particles with $x_+>0$ are almost separated in phase space from those with $x_->0$. When we consider the distribution at $x_+>0$, the constraint $\Sigma_i x_{i-} = 1$ works as a cut off for $x_+\sim 0$, but its exact form is irrelevant. Therefore, we may adopt the approximation

$$\delta(1-\Sigma_i x_{i-}) \sim \Pi_i\, \theta(x_{i+}-\varepsilon), \qquad \varepsilon\sim 0(m_T^2/s), \tag{7}$$

and write $dy=dx/x$ where $x\equiv x_+$ for brevity. Then from Eq.(6) we have

$$P_n(x_1\cdots x_n) \equiv \frac{1}{\sigma_{tot}} \frac{d\sigma_n}{dx_1\cdots dx_n}$$

$$\simeq N_0 \frac{\lambda^n}{n!} \delta(1-\sum_i x_i) \prod_i \frac{\theta(x_i-\varepsilon)}{x_i} \qquad (8)$$

One-particle distribution in n-particle state, $P_n(x)$, and inclusive one-particle distribution $P(x)$ are defined as

$$P_n(x) = \prod_i \int_0^1 dx_i \cdot \sum_j \delta(x-x_j) \cdot P_n(x_1,\cdots x_n),$$

$$P(x) = \sum_n P_n(x).$$

In the approximation $\varepsilon\to 0$, we obtain very simple result

$$P(x) \simeq \lambda x^{-1}(1-x)^{\lambda-1}. \qquad (9)$$

For completeness, let us briefly recapitulate the derivation of Eq.(9).

We may express $P_n(x)$ as

$$P_n(x) = \frac{N_0 \lambda^n}{(n-1)!x} \prod_{i=1}^{n-1} \int_\varepsilon^\infty \frac{dx_i}{x_i} \cdot \delta(1-x-\sum_{j=1}^{n-1} x_j) .$$

Substituting

$$\delta(1-x-\Sigma x_j) = \frac{1}{2\pi}\int_{-\infty}^{\infty} d\xi\, e^{i\xi(1-x-\Sigma x_j)}$$

and performing the integrations over dx_i, we obtain

$$P_n(x) = \frac{\lambda N_0}{2\pi x} \frac{\lambda^{n-1}}{(n-1)!} \int_{-\infty}^{\infty} d\xi\, e^{i\xi(1-x)} [-E_i(-i\xi\varepsilon)]^{n-1},$$

where $E_i(-z)$ is the exponential integral,

$$E_i(-z) = -\int_z^\infty \frac{e^{-t}}{t}\, dt.$$

Summing up over n, we have

$$P(x) \simeq \frac{\lambda N_0}{2\pi x} \int_{-\infty}^{\infty} d\xi\, e^{i\xi(1-x)-\lambda E_i(-i\xi\varepsilon)}$$

$$\simeq \frac{\lambda N_0}{2\pi x} \int_{-\infty}^{\infty} d\xi\, \frac{e^{i\xi(1-x)}}{(i\xi\varepsilon)^\lambda}$$

since $E_i(-i\xi\varepsilon) \simeq \ln(i\xi\varepsilon)$ as $\varepsilon\to 0$. Then we obtain

$$P(x) \simeq \frac{N_0}{\varepsilon^\lambda \Gamma(\lambda)} \frac{\lambda}{x}(1-x)^{\lambda-1}.$$

The overall normalization is $N_0 \simeq \varepsilon^\lambda \Gamma(\lambda)$, in order to satisfy the sum rule

$$\int_0^1 dx\, x\, P(x) = 1.$$

Thus we have reached the result, Eq.(9).

Now, converting the role of x_+ and x_-, we obtain at $x_->0$ where $x_+\sim 0$,

$$P(x_-) \equiv \frac{1}{\sigma_{tot}} \sum_n \frac{d\sigma_n}{dx_-} = \lambda x_-^{-1}(1-x_-)^{\lambda-1}. \qquad (10)$$

Since

$$\frac{dN}{dy} = x_+ P(x_+) = x_- P(x_-),$$

Eqs.(9) and (10) for the forward and backward fragmentation regions $x_+ > 0$ and $x_- > 0$, respectively, are smoothly connected in the central region $x_\pm \sim 0$, giving $dN/dy \simeq \lambda$. Therefore, we may constract an overall expression,

$$\frac{dN}{dy} \simeq \lambda (1-x_+)^{\lambda-1} (1-x_-)^{\lambda-1}, \qquad (11)$$

as an interpolation of Eqs.(9) and (10). In Eq.(11), the divergence of $P(x_\pm)$ as $x_\pm \to 0$ in Eqs.(9) and (10) is automatically avoided. We may further simplify Eq.(11) in terms of the radial variable $\bar{x}$ as

$$\frac{dN}{dy} \simeq \lambda (1-\bar{x})^{\lambda-1}, \qquad (12)$$

where

$$\bar{x} \equiv \frac{2E}{\sqrt{s}} = x_+ + x_-. \qquad (13)$$

Thus, we have obtained simple results expressed as Eqs.(9), (11) or (12) for the inclusive single-particle distribution in the uncorrelated jet model, under the energy momentum constraint in the longitudinal phase space. We note that the fugacity λ gives the hight of the central plateau $dN/dy \simeq \lambda$ at $x_\pm \simeq 0$ and determines the shape of the distribution. Dimensional parameters m_T^2 and

s are hidden in the above expressions, where the scaling relation $m_T^2/s = x_+ x_-$ is implicit. Therefore, with increasing s, the central plateau prolongs as Feynman suggested, resulting the average multiplicity

$$\langle n(s) \rangle = \int dy \, \frac{dN}{dy} \simeq \lambda \ln s + \text{const.} .$$

Similar to the derivation of Eq.(9), Inclusive two particle distribution for a+b → c+d + anything can be obtained at $x_{c+} \equiv x_c > 0$ and $x_{d+} \equiv x_d > 0$ as

$$P(x_c, x_d) = \frac{dN(a+b \to c+d+X)}{dx_c dx_d} = \lambda^2 x_c^{-1} x_d^{-1} (1-x_c-x_d)^{\lambda-1}. \qquad (14)$$

An overall expression can be written as

$$\frac{d^2N}{dy_c dy_d} \simeq \lambda^2 (1-x_{c+}-x_{d+})^{\lambda-1} (1-x_{c-}-x_{d-})^{\lambda-1} \qquad (15)$$

When c and d are produced in forward and backward regions, respectively, Eq.(15) satisfies the factorization

$$\frac{d^2N}{dy_c dy_d} \simeq \lambda^2 (1-x_{c+})^{\lambda-1} (1-x_{d-})^{\lambda-1} \simeq \frac{dN}{dy_c} \frac{dN}{dy_d}$$

since $x_{c-} \sim 0$ and $x_{d+} \sim 0$.

Thus, we have learned "the dynamics of the kinematics" in the longitudinal phase space, in a simple analytic way. More detailed studies, numerical as well as analytic, of the uncorrelated jet model have been carried out incorporating also the p_T spread.[21)]

2.2. Leadership of valence partons —— Kuti-Weisskopf model

In the parton model, a fast moving hadron toward the longitudinal direction is regarded as a non-monochromatic beam of partons collimated to the same direction. Namely, the light-like fraction x_+ of a parton along the hadron momentum defined by

$$k_+ = x_+ P_+ \qquad (16)$$

is distributed in $0<x_+<1$, where k and P are the momenta of the parton and the hadron, respectively. It is assumed that partons are collimated with $k_T \lesssim 0(1\text{GeV})$, and nearly on-mass shell, i.e.,

$$k^2 = k_+ k_- - k_T^2 \lesssim 0(1\ \text{GeV}^2),$$

resulting

$$k_-, k_T \ll k_+ .$$

In the following, we concentrate our attention on the $x_i (\equiv x_{i+})$ distribution.

In the Kuti-Weisskopf model[22], the exclusive n-parton distribution inside a meson is given by

$$P_n(x_1 \cdots x_n) = N_0 \frac{\lambda^{n-2}}{(n-2)!}\, \delta(1-\sum_{i=1}^{n} x_i)\,(x_1 x_2)^A \prod_i \frac{\theta(x_i-\varepsilon)}{x_i}, \qquad (17)$$

where the Kuti-Weisskopf factors x_i^A for valence partons denoted by

i=1 and 2 are introduced so that they have larger shares of the momentum fraction compared with sea partons (gluons and sea quarks) $i \geq 3$. Except for these factors, the above distribution is quite similar to Eq.(8) for the uncorrelated jet model.

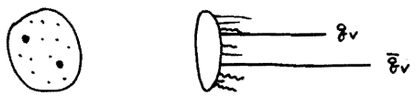

Fig.2. How a meson looks like in the Kuti-Weisskopf model.

Through similar manipulations as in 2.1, we obtain the inclusive distribution of the valence parton

$$P^v(x_i) = \frac{x_i^{A-1}(1-x_i)^{A+\lambda-1}}{B(A,A+\lambda)}, \qquad i=1,2, \qquad (19)$$

where $B(a,b)=\Gamma(a)\Gamma(b)/\Gamma(a+b)$, and the sea distribution

$$P^s(x_s) = \lambda x_s^{-1}(1-x_s)^{2A+\lambda-1}, \qquad (20)$$

where x_s refers to any one of sea partor-

We may obtain the joint distribution of t.. lence partons at x_1 and x_2 as

$$P^{vv}(x_1,x_2) = \frac{\Gamma(2A+\lambda)}{\Gamma(A)^2\Gamma(\lambda)}\,(x_1x_2)^{A-1}(1-x_1-x_2)^{\lambda-1}. \qquad (21)$$

Similarly, other joint distributions such as valence-sea, valence-valence-sea are obtained as

$$P^{VS}(x_1,x_S) = \frac{\lambda x_1^{A-1} x_S^{-1}(1-x_1-x_S)^{A+\lambda-1}}{B(A,A+\lambda)}, \qquad (22)$$

$$P^{VVS}(x_1,x_2,x_S) = \frac{\lambda\Gamma(2A+\lambda)}{\Gamma(A)^2\Gamma(\lambda)} (x_1x_2)^{A-1} x_S^{-1} (1-x_1-x_2-x_S)^{\lambda-1}. \qquad (23)$$

Parton distributions inside a baryon can be obtained by assuming the factors x_i^A for three valence partons, i=1, 2 and 3:

$$P^V(x_1) = \frac{x_1^{A-1}(1-x_1)^{2A+\lambda-1}}{B(A,2A+\lambda)}, \qquad (24)$$

$$P^S(x_S) = \lambda x_S^{-1}(1-x_S)^{3A+\lambda-1}, \qquad (25)$$

$$P^{VS}(x_1,x_S) = \frac{\lambda x_1^{A-1} x_S^{-1}(1-x_1-x_S)^{2A+\lambda-1}}{B(A,2A+\lambda)} \qquad (26)$$

Although deep inelastic scattering only measures single-parton distribution, joint distributions contain more detailed knowledge of the hadron structure. They are utilized in parton recombination model for small p_T hadron production, as we come back in Sect. 4.

Finally, we discuss important characteristics of the Kuti-Weisskopf model.

In the Kuti-Weisskopf type distributions, the kinematical constraint, $\sum_i x_i=1$, and the leading valence effect are built-in. In the formula of inclusive distributions such as above, the exponents of x_i and $(1-x_i...-x_j)$ satisfy the valence counting rule, i.e., the following factors appear in the formula:

$x_i^{n_i A-1}$ and $(1-x_i-\cdots-x_j)^{n_X A+\lambda-1}$,

where n_i=1 for i=valence and n_i=0 otherwise, and n_X is the number of valence partons in the anything state in the inclusive distribution as hadron → i+···+j+anything.

The value of A is determined by the Regge behavior of the valence distribution $P^V(x)\sim x^{-\alpha_R(0)}$ at x~0, as

$$A = 1-\alpha_R(0), \qquad (27)$$

where $\alpha_R(0)$ is the intercept of the vector-tensor trajectory. However, the value A≃0.5 corresponding to $\alpha_R(0)\simeq 1/2$ is quite insufficient to make the sea distribution (25) strongly damped as x→1, since it is different from the valence distribution only by factor $(1-x)^A$. Recent data on nucleon structure function indicate that the sea-quark distribution behaves as $xP^S(x)\sim(1-x)^{6\sim9}$, while $xP^V(x)\sim x^{0.5\sim1}(1-x)^{3\sim4}$.[23] In order to accomodate with the data, various versions of the Kuti-Weisskopf model have been proposed by assuming more detailed form of the leading factors or phenomenologically changing the inclusive parametrization.[24]

Anyway, sea partons in the Kuti-Weisskopf model and its versions are completely uncorrelated except for the overall momentum conservation. Therefore, "the temperature of the sea-partons" is very high, in a vague sense that the correlation is absent among them similar to the ideal gas limit of real gas at high temperature. However, there are strong indications of the correlation and ordering

among sea quarks concerning the flavor structure of the hadron reactions. We now proceed to discuss "a cold and adiabatic evolution of the cloud" from fast moving quark.

3. Quark-chain model and cascade structure

3.1. Quark cascade model

Let us consider meson distributions in a quark jet in a process such as $e^+e^- \to q\bar{q} \to$ hadrons. In the quark cascade model,[9~11] mesons are emitted through the cascade of basic subprocess $q(x) \to$ meson+$q'(x')$ as shown in Fig.3, where x and x' are the light-like fractions of the quark momenta with respect to the initial quark. Assuming that the momentum separation of the subprocess depends only on the ratio x'/x, we obtain the following recurrsive equation for the meson distribution:

$$g(z) = k(z) + \int_z^1 \frac{dx}{x}\, g\left(\frac{z}{x}\right)\, f(x), \tag{28}$$

where g(z) is the inclusive meson distribution with light-like fraction z of the initial quark in the phase space dz/z, while k(z) and f(x) are irreducible probability distributions of a meson and a child quark, respectively, satisfying $k(z)/z=f(x)/x\big|_{x=1-z}$, i.e.,

$$k(z) = \frac{z}{1-z}\, f(1-z)\,. \tag{29}$$

The recurrsive relation can be described as Fig.4, and follows from the relation of probability density in dz,

$$\frac{g(z)}{z} = \frac{k(z)}{z} + \int_0^1 dx\, \frac{f(x)}{x} \int_0^1 dy\, \frac{g(y)}{y}\, \delta(z-xy).$$

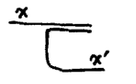

Fig. 3.

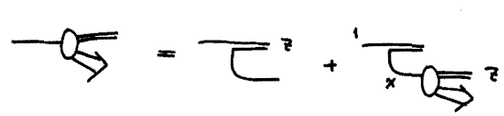

Fig. 4.

For a simple case

$$f(x) = \lambda x^{\lambda}, \tag{30}$$

we obtain

$$g(z) = \lambda(1-z)^{\lambda-1}\,, \tag{31}$$

which is the same form as the distribution zP(z) in the uncorrelated jet model, Eq.(9). However, the mesons in the final state are strongly correlated as seen from Fig.4, since the ordering in the momentum fraction follows the order of emission on the average. Especially, the first meson containing initial quark is relatively fast. We may introduce different flavors of the quarks, putting $\lambda=\lambda_u+\lambda_d+\lambda_s+\cdots$. Then, the above ordering can be easily seen from the flavor structure of the final state. For example, K^+ and K^- are strongly correlated than K^+ and K^- in the rapidity space, where rapidity Y is given by $Y= \ln p_+/m_T = \ln z + \ln P_+/m_T$, since two K^+ cannot be produced succesively. Thus, we may regard the meson distribution in the quark cascade model as a consequence of

"the evolution of cold meson cloud", keeping the memory of how they are produced.

The above properties of the ordering is a general characteristics of the cascade structure. The solution of Eq.(28) can be obtained for arbitrary f(x) by invoking the Mellin transformation technique. Namely, in terms of

$$\tilde{f}(J) = \int_0^1 dz z^{J-2} f(z), \tag{32}$$

and so forth for $\tilde{q}$ and $\tilde{k}$, we can rewrite Eq.(28) as

$$\tilde{g}(J) = \tilde{k}(J) + \tilde{f}(J)\tilde{g}(J), \tag{33}$$

and obtain the solution

$$\tilde{g}(J) = \tilde{k}(J) / (1-\tilde{f}(J)), \tag{34}$$

$$g(z) = \frac{1}{2\pi i} \int_{c-i\infty}^{c+i\infty} dJ \cdot z^{-J} \tilde{g}(J), \tag{35}$$

where c is an appropriate real positive constant ensuring the convergence of the integral.

If the condition

$$\int_0^1 \frac{dx}{x} f(x) = 1 \tag{36}$$

is satisfied, the cascade process proceeds with the probability one, so that an isolated quark does not come out with finite x in the final state. Therefore, this condition for the quark jet in the

e^+e^- annihilation corresponds to the quark confinement.

The quark cascade model was also applied to hadronic processes by Fukuda and Iso,[9] assuming the constituent quark structure of hadrons. They have relaxed the above condition so as to introduce the recombination probability with other cascading quarks. (see Sect.8.1).

3.2.Quark chain model

In the naive parton model, the hadronization process of a quark jet is treated as if it is the decay of a quark into hadrons, leaving a very slow quark which will afterwards join, in the case of the e^+e^- annihilation, with a slow antiquark from the antiquark jet. However, the evolution of the quark jet is not an isolated phenomenon of the quark decay, but it must be related to the color confinement mechanism in some essetial way.

In reality, it may be a very complicated process involving fragmentation and recombination of quarks and gluons such as shown in Fig.5. Still, if we notice the net flavor flow among final hadrons and initial quark and antiquark in the case of $e^+e^- \to q\bar{q} \to$ hadrons, we may reasonably assume the quark chain structure as shown in Fig.6, in accordance with the IOZ rule and the short range flavor correlation in the rapidity space in the frame where q and $\bar{q}$ are colinear.[12]

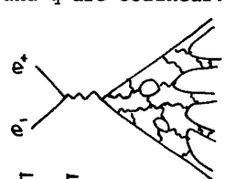

Fig.5.

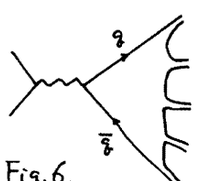

Fig.6.

In the above, the pair of momenta of q and $\bar{q}$ gives the driving force to produce multiparticle final state, since $(p_q+p_{\bar{q}})^2=Q^2>0$, even if we may treat the quark as exactly massless and on-shell. In contrast, massless particle cannot decay into massive particles spontaneously.

As an underlying mechanism for the formation of the quark-chain, we may imagine that the color electric flux between separating triplet color and its complimentary color induces polarization of $q\bar{q}$ pairs, and then they recombine into hadrons attaining the color neutralization, as suggested by Casher, Kogut and Susskind.[25]

So much for the philosophy of the quark chain model, let us now consider the momentum distribution of produced hadrons in the process $e^+e^- \to q\bar{q} \to$ hadrons. Considering the light-like fractions $x_\pm$ of a hadron with respect to the momenta of q and $\bar{q}$ as in Sect.2.1, we may assume the cascade structure of x_+ from the parent quark and that of x_- from the parent antiquark. This assumption implies a dual partition of parents' momenta among final hadrons, in the sense that the quark chain emitting mesons between initial quark and antiquark can be regarded at the same time as the quark cascade from the initial quark concerning the fraction x_+, and also as the antiquark cascade in the opposite direction concerning x_-, as illustrated in Fig.7. Since $x_+x_-=m_T^2/s$, we may easily see that the ordering in x_+ implies those in x_- in the opposite directions.

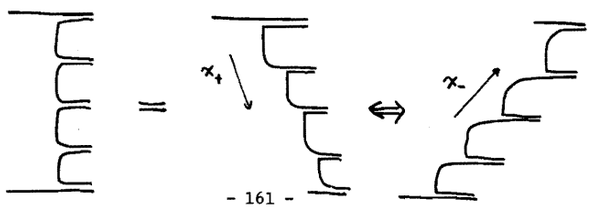

Fig.7.

For the inclusive single hadron distribution, the above assumption leads to

$$\frac{dN}{dy} = \frac{g(x_+)g(x_-)}{g(0)} , \tag{37}$$

which reduces to $dN/dy \sim g(x_+)$ at $x_+>0$. For the case of $f(z)=\lambda z^\lambda$, we obtain

$$\frac{dN}{dy} \simeq \lambda(1-x_+)^{\lambda-1}(1-x_-)^{\lambda-1} \simeq \lambda(1-\bar{x})^{\lambda-1} .$$

If we do not inquire into the quantum number structure of final states, we obtain in this case the same form of inclusive two hadron distribution as Eq.(15) in the uncorrelated jet model.

As an illustration to distinguish the quark chain model from naive fragmentation model, let us consider the upsilon decay into hadrons through three gluons. We assume that each gluon fragments into a $q\bar{q}$ pairs which forms color octet, and then hadrons are produced from color singlet $q\bar{q}'$ pairs where q and $\bar{q}'$ originate from different gluons, as shown in Fig.8. The circulation of the triplet colors is described in Fig.9. In this model we may predict various properties of the upsilon $\to$ hadrons using the data on $e^+e^- \to q\bar{q} \to$ hadrons as inputs.

Fig.8.

Fig.9.

We note that the hadronic final state in the upsilon decay is not colinear as in $e^+e^- \to q\bar{q} \to$ hadrons, but coplanar in the plane determined by the momenta of three gluons, under the assumption of colinearity of gluon $\to q\bar{q}$.

Now let us consider the momentum distribution of hadrons from a $q\bar{q}'$ pair, which is not at rest in the rest system of the upsilon. We can easily handle this problem without complicated Lorentz boost, by utilizing the Sudakov parametrization of a hadron momentum p:

$$p_\mu = \xi a_\mu + \eta b_\mu + \tilde{c}_\mu, \tag{38}$$

where a and b denote the momenta of parents q and $\bar{q}'$, respectively, satisfying $a^2=b^2=0$, and

$$a\tilde{c} = b\tilde{c} = 0. \tag{39}$$

We note that ξ,η and $\tilde{c}^2$ are all Lorentz scalars given by

$$\xi = 2pb/s_{ab}, \qquad \eta = 2pa/s_{ab}, \qquad \tilde{c}^2 = m_h^2 - \xi\eta s_{ab}, \tag{40}$$

where $s_{ab}=(a+b)^2=2ab$. From these expressions, we can easily see that ξ,η and $-\tilde{c}^2$ coincide with x_+,x_- and p_T^{*2} in the CMS of $q\bar{q}'$ with longitudinal axis directing the momentum of q. For completeness we show in Fig.10 how to perform the Lorentz boost from an arbitrary system to the CMS.

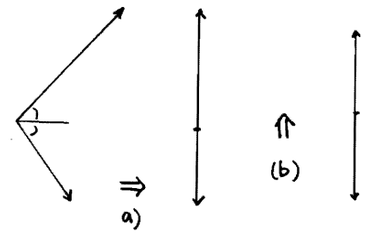

Fig.10. a) Arbitrary system → colinear system.
b) Colinear system → CMS.

Thus, the properties of Lorentz invariant distribution in terms of ξ,η and $\tilde{c}^2$ can be easily inferred in the CMS of $q\bar{q}'$, e.g.,

$$\frac{Ed^3N}{dp^3}(q\bar{q}' \to hX) = \frac{E^*d^3N}{dp^{*3}}(q\bar{q}' \to hX) = \rho(\xi,\eta;p_T^{*2}). \tag{41}$$

Similarly, we may parametrize inclusive two-hadron distribution $q\bar{q}' \to h_c h_d X$ as

$$\frac{E_cE_dd^6N}{dp_c^3dp_d^3} = \frac{E_c^*E_d^*d^6N}{dp_c^{*3}dp_d^{*3}} = \rho(\xi_c,\xi_d,\eta_c,\eta_d;\ p_{cT}^{*2},\ p_{dT}^{*2}). \tag{42}$$

An immediate and important consequence of the hadron distribution with $p_T^{*}+m_h^2 \ll s_{ab}$ is that they are collimated along q or $\bar{q}'$ according to $\xi>0$ or $\eta>0$, respectively, since $\xi\eta=(m_h^2+p_T^{*2})/s_{ab}\approx 0$. Therefore, at sufficiently high s_{ab}, final hadrons distribute as if they are independent fragments of q and $\bar{q}'$ as told in the naive fragmentation model. In contrast to the naive model, however, the quark chain model provides a smooth connection of the central region with the fragmentation regions of q and $\bar{q}'$.

Therefore, the average multiplicity depends on s_{ab} which is affected by the opening angle of a and b, which is not the case in the naive model. The average multiplicity in the Υ decay is consistent with the data in this model,[13] in contrast to too high result of the naive fragmentation model.

A straightforward extention of the quark-chain model to $e^+e^- \to q\bar{q}G \to$ hadrons may be described by a webbed foot diagram shown in Fig.11. The quark chain model and similar approaches based on dual-sheet picture[26] have been applied to hadronic and lepton-hadron reactions, where the diagrams such as shown in Figs.12 and 13 have been considered. We will come back to such processes in section 7.

Fig. 11.

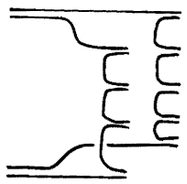

Fig. 12.

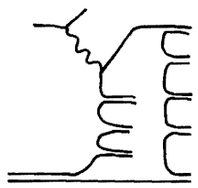

Fig. 13.

3.3. Resonances, fireballs and the parent-child relation

In the previous arguments in this section, we have discussed the distribution of hadrons directly produced from the quark chain. Rigorously speaking, what are produced directly are not restricted to stable hadrons. They may be hadrons, resonances and fireballs, considered as color neutral clusters of $q\bar{q}$ (or qqq) plus gluons

characterized by finite mass and limiting temperature. The mass of a fireball (or cluter) is estimated to be 1~2 GeV, and average decay multiplicity 3~5.[27]

In hadronic reactions, it is reported that only 30% of pions are produced directly, while others are decay products of resonances. Here we discuss briefly the distribution of indirectly produced particles through the decay of a resonance (or a fireball), given its distribution $XdN/dX=G(X)$ in terms of the light-like fraction X with respect to some jet source. Since the decay is an on-shell process, the fraction

$$z = \frac{(e+p)_{child}}{(E+P)_{parent}} = \frac{m_T e^Y}{M_T e^Y} \tag{43}$$

is invariant under longitudinal boost. Therefore, we may obtain invariant distribution $zdN/dz=F(z)$ from the phase space integral. The final result of the particle distribution with respect to the jet source is the convolution (Fig.14),

$$g(x) = \int_0^1 dX G(X) \int_0^1 dz F(z) \delta(x-Xz)$$

$$= \int_x^1 \frac{dX}{X} G(X) F(\frac{x}{X}). \tag{44}$$

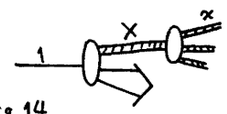

Fig. 14.

Recently, it was noted that F(z) can be approximated in may cases by the form

$$F(z) = F_0 z^A (1-z)^B, \tag{45}$$

where F_0, A and B are constant to be adjusted according to the nature of the decayed state.[28]

If we may put

$$G(X) = G_0 x^C (1-X)^D, \tag{46}$$

we obtain, for C<A,

$$g(x) = F_0 G_0 x^C (1-x)^{B+D+1} \tilde{q}(x), \tag{47}$$

where $\tilde{g}(x)$ is a mild function for 0<x<1, written as

$$\tilde{g}(x) = \int_0^1 \frac{dt\, t^B (1-t)^D}{[1-(1-x)t]^{1+C+D-A}} . \tag{48}$$

We see from Eq.(47) that directly produced particle tends to dominate over indirect one as $x \to 1$, due to the penalty of extra factor $(1-x)^{B+1}$.

4. Chromodynamic cascade shower of quarks and gluons

Generally speaking, there are plenty of cascade processes in nature such as air shower of cosmic rays, reactions inside the nuclear power plants, and so on. They may be classified into two categories: recurrsive chain type and branching shower type, or, in other words, ivy and tree types, such as shown in Figs.15 and 16. Of cource, the quark chain model in Sect.3 belongs to the former. On the other hand, the jet picture in perturbative QCD approach

belongs to the latter, regarded as a cascade shower involving quarks and gluons. In this section we briefly discuss this picture.

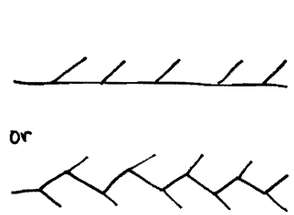

Fig.15. Chain type cascade.

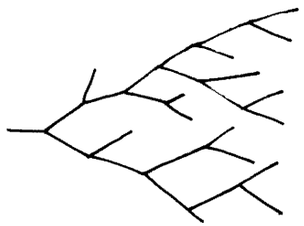

Fig.16. Shower type cascade.

4.1. Parton picture in QCD

First of all, the parton picture in QCD is different from naive one with scaling distribution, but it belongs to the scale invariant parton model[29] in which definition of the parton changes with the resolution scale. For instance, a quark parton at certain Q_0^2 turns out to be a quark plus a gluon or more with increasing resolution Q^2, which is the momentum squared characterizing the hard subprocess. Therefore, parton distributions inside a hadron changes with Q^2, as described by the Altarelli-Parisi evolution equations (see Fig.17):[30]

$$\begin{aligned} \frac{\partial q^i(x,t)}{\partial t} &= \frac{\alpha(t)}{2\pi}\int_x^1 \frac{dy}{y}\left[q^i(y,t)P_q^q\left(\frac{x}{y}\right) + G(y,t)P_G^q\left(\frac{x}{y}\right)\right], \\ \frac{\partial G(x,t)}{\partial t} &= \frac{\alpha(t)}{2\pi}\int_x^1 \frac{dy}{y}\left[\sum_{i=1}^{2f} q^i(y,t)P_q^G\left(\frac{x}{y}\right) + G(y,t)P_G^G\left(\frac{x}{y}\right)\right], \end{aligned} \tag{49}$$

where the index i runs over quarks and antiquarks of all flavors, and the evolution variable is defined by $t=\ln Q^2/Q_0^2$, which

determines the coupling strength in the leading log approximation as

$$\alpha(t) = \frac{\alpha(0)}{1+b\alpha(0)\ln(Q^2/Q_0^2)}, \qquad b = \frac{33-2N_f}{12\pi}, \tag{50}$$

N_f being the number of flavors. The branching functions are given by the lowest order emission diagrams in QCD such as $q(p) \to q(zp)+G$, with the following results:

$$\begin{aligned} P_q^q(z) &= \frac{4}{3}\cdot\left(\frac{1+z^2}{1-z}\right)_+ , \\ P_q^G(z) &= \frac{4}{3}\,\frac{1+(1-z)^2}{z} , \\ P_G^q(z) &= \frac{N_f}{2}\left[z^2+(1-z)^2\right] , \\ P_G^G(z) &= 6\left[\frac{1-x}{x} + \left(\frac{x}{1-x}\right)_+ + x(1-x) - \frac{\delta(1-x)}{12}\right] - \frac{N_f}{3}\,\delta(1-x) , \end{aligned} \tag{51}$$

where the distribution $(f(z))_+$ is defined by

$$\int_0^1 (f(z))_+ \, g(z)dz = \int_0^1 f(z)\left[g(z)-g(1)\right] dz. \tag{52}$$

Thus, from initial distributions at sufficently large Q_0^2 in the leading log approximation, we may obtain evolved distributions at Q^2. Standard technique to solve the evolution appeals to the Mellin trnasformation, as briefly discussed for the QCD jets in the next subsection.

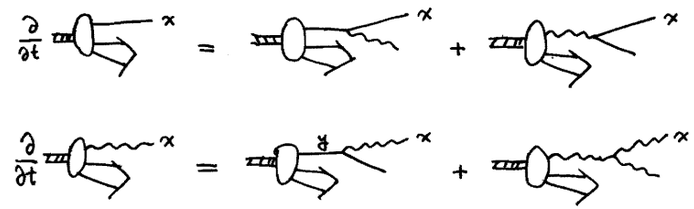

Fig.17. Altarelli-Parisi evolution equation.

4.2. Jet picture in QCD

let us now consider a jet from a parton which is kicked out by a hard subprocess characterized by Q^2. Since the definition of partons depends on Q^2 in QCD, the properties of the jet changes also with Q^2. Instead of considering a jet of hadrons, we may look at it as a jet of partons defined at $Q_0^2 \ll Q^2$, bypassing the confinement problem related to hadronization.

In the perturbative QCD approach, the kicked out parton at Q^2 can be regarded as a jet of partons with degraded resolution $Q_0^2 < Q^2$, given by the branching process reciprocal to the evolution of the parton distribution with Q^2 such as shown in Fig.18.

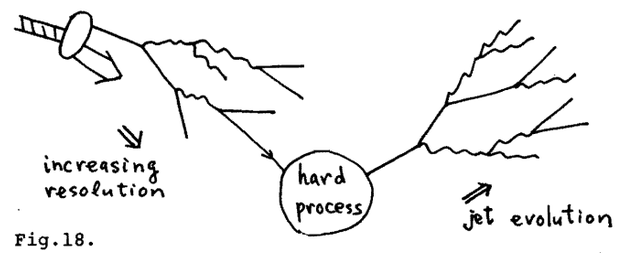

Fig.18.

Inside a jet with Q^2, single parton distribution $D^{a\to b}(x,t)$ for $a(p)\to b(xp)+$anything, where b is defined at fixed Q_0^2, satisfies the evolution equation

$$\frac{\partial}{\partial t} D^{a\to b}(x,t) = \frac{\alpha(t)}{2\pi} \sum_i \int_x^1 \frac{dz}{z} D^{a\to i}(\frac{x}{z},t) P_i^{\ b}(z), \qquad (53)$$

where $t=\ln(Q^2/Q_0^2)$, and $P_i^{\ b}(z)$ are the same as in Eq.(51). Converting into the moment space,

$$\mathbb{D}_n(t) = \int_0^1 dx\, x^n D(x,t), \qquad \mathbb{A}_n = \int_0^1 dz\, z^n P(z). \qquad (54)$$

and using the double log variable,

$$Y = \frac{1}{2\pi b} \ln\left[1+\alpha_s b \ln\frac{Q^2}{Q_0^2}\right], \qquad (55)$$

we may rewrite Eq.(53) as

$$\frac{dD_n^{a\to b}(Y)}{dY} = D_n^{a\to i}(Y) A_n^{i\to b}. \qquad (56)$$

The solution of Eq.(56) is

$$\mathbb{D}_n(Y) = \mathbb{D}_n(0) \exp(\mathbb{A}_n Y),$$

$$= \mathbb{D}_n(0) \sum_{\ell=0}^{\infty} \frac{(\mathbb{A}_n Y)^\ell}{\ell!}. \qquad (57)$$

Eq.(57) can be interpreted as summing up all possible pathes in all possible branching processes, as illustrated in Fig.19.

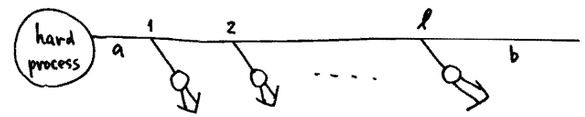

Fig. 19.

Furthermore, multiparton distributions inside a QCD jet can be computed as explored by Konishi, Ukawa and Veneziano.[31] For instance, inclusive two parton distribution $D^{a\to bc}(x,y;Y)$ for $a(p)\to b(xp)+c(yp)+$anything satisfies the equation(see Fig.20) as

$$D^{a\to bc}(x,y;Y) = \int_0^Y dY' \int_{\max(x,y)}^1 dw D^{a\to i}(w,Y-Y') \cdot dz dz' P^{i\to jk}(z,z') \times \frac{1}{wz} D^{j\to b}(\frac{x}{wz},Y') \frac{1}{wz'} D^{k\to c}(\frac{y}{wz'},Y'), \qquad (58)$$

where

$$P^{i\to jk}(z,z') = \delta(z+z'-1) P^{i\to j}(z). \qquad (59)$$

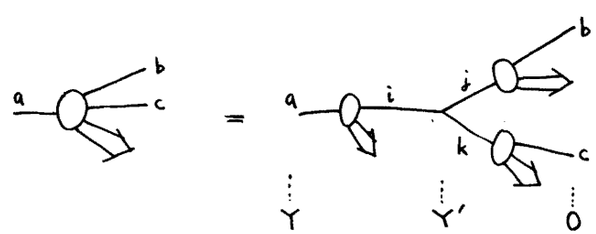

Fig.20. Two parton distribution $a\to c+d+$anything.

In terms of double moments,

$$D_{m,n}(Y) = \int_0^1 dx \int_0^1 dy\ x^m y^n D(x,y;Y),$$
$$P_{\ell,\ell'} = \int_0^1 dz \int_0^1 dz'\ z^\ell z'^{\ell'} P(z,z'), \qquad (60)$$

We may rewrite Eq.(58) as

$$D^{a\to bc}_{mn}(Y) = \int_0^Y dY'\ D^{a\to i}_{m+n}(Y-Y') P^{i\to jk}_{mn} D^{j\to b}_{m}(Y') D^{k\to c}_{n}(Y'). \qquad (61)$$

Introducing E-variable conjugate to Y as

$$\bar{D}(E) = \int_0^\infty dY\, e^{-EY} D(Y), \qquad (62)$$

we may further rewrite Eq.(61) as

$$D^{a\to bc}_{mn}(E) = \langle a|(E-\mathbb{A}_{m+n})^{-1}|i\rangle P^{i\to jk}_{mn} \langle j,k|(E-\mathbb{A}_m-\mathbb{A}_n)^{-1}|b,c\rangle, \qquad (63)$$

where $\langle j,k|(\mathbb{A}_m)^\ell(\mathbb{A}_n)^{\ell'}|b,c\rangle = \langle j|(\mathbb{A}_m)^\ell|b\rangle\langle k|(\mathbb{A}_n)^{\ell'}|c\rangle$ is implied. Thus, the moment of the inclusive distribution in the E space satisfies a relation analogous to the amplitude in old fashioned perturbation theory, where inclusive distributions are regarded as Green's functions, and moments are conserved at the vertex given by the QCD branching functions. These results are generalized for inclusive multiparton distributions and summarized as an algorithm for QCD jets by KUV.[31] Some result of application are the followings:

1) Gluon jets are softer in x and wider in p_T than quark jets.

Quantitatively, the ratio of the multiplicity is determined by the color factor asymptotically as

$$\frac{\langle n\rangle_{G\text{-jet}}}{\langle n\rangle_{q\text{-jet}}} \to \frac{C_A}{C_F} = \frac{9}{4}.$$

2) Multiplicity distribution exhibits long range correlations as

$$\frac{D}{\langle n\rangle} \approx \frac{\sqrt{\langle n(n-1)\rangle - \langle n\rangle^2}}{\langle n\rangle} = \begin{cases} 1/\sqrt{3} & \text{for G-jet,} \\ \sqrt{3}/2 & \text{for q-fet.} \end{cases}$$

3) The transverse structure of QCD jets is quite broad, as

$$\langle p_{T_{1,2}}^2\rangle \sim \langle x_1 x_2\rangle Q^2 \alpha_s(Q^2),$$

for the relative p_T of two partons in the jet. Here, the p_T structure can by treated because it is regarded as the merkmal of the virtuality Q^2, although the formulation is explicitly concerned with longitudinal structure.

In the above picture of QCD jets, as branching evolution of partons, we are not dealing with the hadronization problem, i.e., how partons recombine into hadrons without leaving colored quanta in the final state. Still, it is possible to show within perturbative approach that the QCD jets prepare the condition of confinement, in the sense that they evolve to form color singlet clusters with finite mass, irrespective to initial Q^2 as shown in Fig.21. This result found by Amati and Veneziano is called pre-confinement.[32]

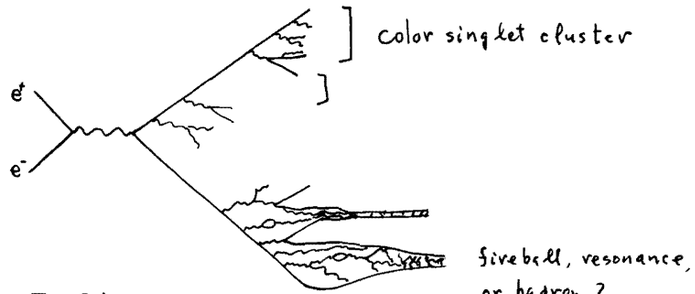

Fig. 21.

Finally, it should be stressed that the angular or transverse profile of QCD jets are qualitatively different from naive parton jets of limited transverse momentum, as first noted by Stermann and Weinberg.[33] First subtle evidence has been reported from PETRA experiments as the discovery of the $q\bar{q}G$ components in $e^+e^- \to$ hadrons.[6]

5. Parton recombination models for spectator jets

As a simple approach to relate parton distributions inside a hadron with the inclusive hadron spectra in soft hadronic reactions, we now discuss quark recombination models for hadron production.

5.1. Meson production

It has been observed that the inclusive x distributions of π^+ and π^- in pp collisions are very similar to the u and d quark-parton distributions inside a proton measured in deep inelastic scattering.[34]

Since $\pi^+ \sim u\bar{d}$ and $\pi^- \sim d\bar{u}$, this similarity indicates the important role of valence quarks $\sim uud$ inside a proton.

As a model to embody this similarity, Das and Hwa[15] proposed a parton recombination model, as described in Fig.22 for pp collisions. Namely, an energetic meson in the fragmentation region is produced by recombination of a valence quark distributing as before the collision, and an antiquark which is created from an excited gluon. Here, it is presupposed that valence quarks pass through in the collision without interacting strongly, while gluons surrounding them become turbulent on account of strong interaction during the collision.

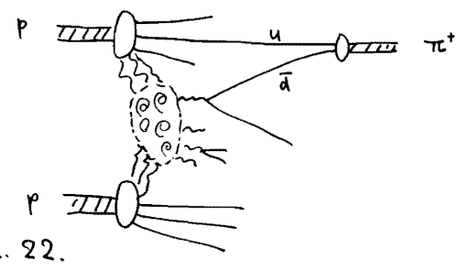

Fig. 22.

The longitudinal distribution is obtained as follows ($x \equiv x_+ \simeq x_{||}$):

$$\frac{x dN}{dx} = \int F(x_1, x_2) R(x_1, x_2; x) \frac{dx_1}{x_1} \frac{dx_2}{x_2} \qquad (64)$$

where $F(x_1, x_2)$ is the two-parton distribution function in the beam side just after the collision but before the hadronization, and $R(x_1, x_2; x)$ is the recombination function for $q(x_1) + q(x_2) \to$ meson ($x = x_1 + x_2$). For $pp \to \pi^+ X$, the following forms were adopted:

$$F(x_1,x_2)=F_u(x_1)F_{\bar{d}}(x_2)\rho(x_1,x_2),$$

$$\rho(x_1,x_2)=\beta\cdot(1-x_1-x_2)^{2k-1}\theta(1-x_1-x_2), \tag{65}$$

where $F_u(x_1)$ is the u-parton distribution measured in deep inelastic scattering, and

$$F_{\bar{d}}(x_2) = C_{\bar{d}}\cdot(1-x_2)^7 , \tag{66}$$

while

$$R(x_1,x_2;x)=R(\xi_1,\xi_2)\delta(\xi_1+\xi_2-1), \qquad \xi_i=x_i/x,$$

$$R(\xi_1,\xi_2) = \alpha_M\cdot(\xi_1,\xi_2)^k , \tag{67}$$

with the values k=1, $\alpha_M\beta=4.3$ which is within the constraint $\alpha_M<6$ and the expectation $\beta\sim1$, and $C_{\bar{d}}=0.4$ which is somewhat enhanced compared with the sea quark distribution measured in deep inelastic scattering, a reasonable fit to the data at large x(>0.5) was obtained.

Here I make a few comments. First, Eq.(65) for the joint distribution function is very questionable in its construction. The behavior of $\rho(x_1,x_2)$ at $x_1+x_2\sim1$ was obtained from the penalty to put two valence quarks in the wee region. Therefore, Eq.(65), with $F_u(x_1)$ as the u-quark distribution which is also subject to the same penalty, contains double counting. Second, the value k=1 was <u>not</u> in agreement with the dimensional counting, which gives

k=3 as the minimum number of quarks udd in the anything state. Third, the value of α_M may be quite small compared with its upper limit, which corresponds to the configuration that the produced meson is composed of bare $q\bar{q}$ without gluons, since half of the energy of a hadron seems to be carried by gluons. In addition to the recombination of bare $q\bar{q}$, we may expect that many gluons take part in pushing the produced meson to large x.

As an alternative to Eq.(65), the two-parton distribution given by the Kuti-Weisskopf model was also employed by DeGrand and Miettinen, in discussing associated meson distribution with the Drell-Yan process.[35] Since the sea quark distribution in the Kuti-Weisskopf model is not soft enough, a detailed modification of it was considered and applied to the recombination model by Texas group.[36]

Prior to the flourishing of the recombination models such as above, the quark fusion model was proposed by Biyajima and Miyamura,[37] and explored by Bonn group.[38] This is an extension of the Drell-Yan mechanism for massive photon(→lepton pair) production to the meson production as follows:

$$\frac{dN}{dY} \propto C_1 f_q(x_+)f_{\bar{q}}(x_-) + C_2 f_{\bar{q}}(x_+)f_q(x_-) \tag{68}$$

$$\longrightarrow C_1 f_q(x_+)f_{\bar{q}}(0) , \qquad \text{for } x_+>0 \quad \text{in } pp\to\pi X.$$

Thus, the longitudinal distribution is almost proportional to the quark-parton distribution in this model. Although the fusion mechanism may be relevant for massive hadron production such as J/ψ, it is not very plausible that the meson production in certain

fragmentation region is dominated by fusion of q and $\bar{q}$ from different hadrons colliding. Actually, the impulse approximation for the fusion picture breaks down if the produced meson mass is not large enough, since one of x becomes too small.

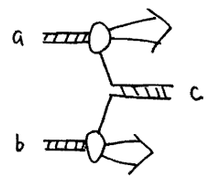

Fig.23. Fusion model for a+b→c+anything.

5.2. Baryon production

As a pioneering work to apply the quark-gluon dynamics to low p_T hadron reaction, Pokorski and Van Hove proposed in 1974 a recombination model for pp→pX.[16] This was based on the observation that the same average 0.5 is found for the elasticity of the leading proton distribution from the proton beam and the total momentum fraction of quark-partons inside the proton. Presupposing that only the glues of colliding protons interact strongly and turn into multiparticle final state while quarks pass through and recombine into protons or its excited states as illustrated in Fig.24, they proposed the following for the (excited) proton distribution:

$$\frac{dN}{dx} = \int P^{vvv}(x_1,x_2,x_3)\ \delta(x-x_1-x_2-x_3)\,dx_1dx_2dx_3, \qquad (69)$$

where $P^{vvv}(x_1,x_2,x_3)$ is the joint valence distribution such as

$$P^{vvv}(x_1,x_2,x_3) = \frac{\text{const.}}{x_1^2+x_2^2+x_3^2}, \qquad x_1+x_2+x_3<1 . \qquad (70)$$

The single valence-quark distribution is obtained as (denoting i=1 for the d-quark in the proton, for simplicity)

$$P^v(x_1) = \int_0^{1-x_1} dx_2 \int_0^{1-x_1-x_2} dx_3\ P^{vvv}(x_1,x_2,x_3) , \qquad (71)$$

which gives a reasonable description of the deep inelastic data although the fall off $P^v(x_1)\sim(1-x_1)^2$ as $x_1\to 1$ is too mild.

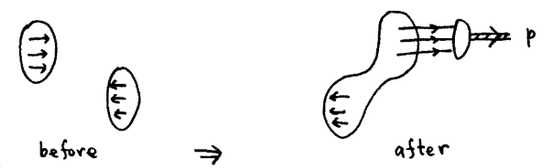

Fig. 24.

The joint distribution (70) gives the flat proton distribution dN/dx=constant, in agreement with the data. However, it should be noted that the quantum number structure of the inclusive distribution indicates that the flat behavior is due to the contribution that two valence quarks of the beam emerge in one baryon, common to pp→nX and ΛX, while the contribution that three valence quarks in one baryon give diffractive peak at x~1, as illustrated in Fig.25.[39]

If we rewrite Eq.(69) as Eq.(64), the recombination function is written as

$$R(x_1,x_2,x_3) = \delta(1-\xi_1-\xi_2-\xi_3) , \qquad \xi_i=x_i/x , \qquad (72)$$

which implies that all of the valence quarks recombine into one (excited) proton with the probability one. Recently, an estimate of this probability was obtained to be 0.35~0.4, while the probability 0.6~0.5 for two valence quarks in one baryon, from an analysis of hyperon productions in pp collisions.[40]

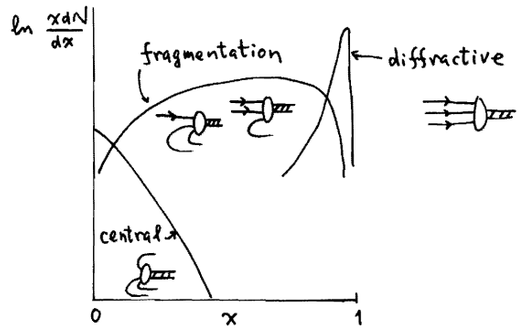

Fig.25. Classification of baryon distributions.

Recently, Ranft discussed the leading proton distribution triggering a large p_T meson or a massive dilepton,[41] generalizing the recombination model of Pokorski and Van Hove. He put

$$R(x_1,x_2,x_3;x) = 120\xi_1\xi_2\xi_3\delta(\xi_1+\xi_2+\xi_3-1) \ , \qquad (73)$$

$$p^{VVV}(x_1,x_2,x_3) = \beta_p \cdot p^V(x_1)p^V(x_2)p^V(x_3)(1-x_1-x_2-x_3)^\gamma \ . \qquad (74)$$

although the above form of three valence distribution is subject to the criticism mensioned before, it was claimed that the value $\gamma=-0.3$ gives acceptable approximation for single valence distribution. A reasonable fit was obtained for the British-Scandinabian-French data of large p_T meson trigger.[42]

Thus, the parton recombination picture is still in some midway of its development. Anyhow, it is extremely interesting to explore joint parton distributions not measured in deep inelastic scattering.

6. Dressed quark picture and fragmentation models

We have seen that the role of gluons bearing half of the energy momentum of a hadron is disregarded in the parton recombination models, except as the source of the $q\bar{q}$ pair creation. It is quite possible, however, that soft hadron reactions are described not by independent partons but in terms of dressed quarks with gluon clouds. We may regard the additive quark picture for multiparticle production shown in Fig.26 as a realization of this viewpoint.[43] The additive quark picture, giving $\sigma_{tot}(MB)/\sigma_{tot}(BB)\sim 2/3$, was also applied to give the production rate of various mesons in the fragmentation region.[44] Now we discuss the problem of longitudinal distributions in this picture.

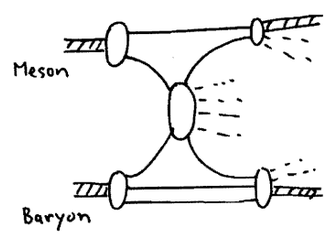

Fig.26. Additive quark picture for multiparticle production.

6.1. Dressed quark distribution

If a baryon is regarded as an additive system of three dressed quarks, which are called "constituent quarks", the baryon momentum is shared among themselves. Therefore, we have the joint distribution as

$$P^{VVV}(x_1,x_2,x_3) = F(x_1,x_2,x_3)\delta(1-x_1-x_2-x_3) \ . \qquad (75)$$

A simple choice may be

$$F(x_1,x_2,x_3) = \frac{\Gamma(3A)}{\Gamma(A)^3}(x_1\ x_2\ x_3)^{A-1} \ , \qquad (76)$$

which gives

$$P^V(x_1) = \frac{x_1^{A-1}(1-x_1)^{2A-1}}{B(A,2A)} \ . \qquad (77)$$

Obviously, we have the equi-partition of x on the average, $\langle x_i\rangle=1/3$, as in the naive quark model with non-relativistic motion. However, the distribution in the full range of $0<x_i<1$ may be taken as a result of highly relativistic internal motion. The above form is adopted in many papers,[9,17,45] but with different values of A, as we discuss later.

Previously, Altarelli et al. derived the constituent quark distribution in the nucleon from the broken $SU(6)_w \otimes O(3)$ scheme, regarding the constituent quark as a cluster of partons.[46]

The result was rather complicated. Kanki applied the Kuti-Weisskopf type model for the parton distribution inside each constituent quark, consisting of one valence quark-parton and sea of quarks and gluons.[17] Taking the convolution of them with constituent quark distribution (77) with A=2, he obtained parton distributions inside a nucleon. The behavior of sea quark distribution at large x is too close to that of valence quark distribution. As an alternative in the constituent quark picture, Hirose and Kanki considered multiperipheral chain as the dress of the constituent quark, and explored phenomenological consequences.[47]

On the other hand, in the context of the QCD evolution picture, it was suggested that the constituent quark itself is a parton looked at with course resolution.[48]

6.2. Meson production in fragmentation models

In the dressed quark picture, the meson distribution in pp collisions at large x is often attributed to the fragments of constituent quarks given by

$$\frac{dN}{dx} = \int_x^1 \frac{dz}{z}\ P^V(\frac{x}{z})D_Q^M(z) \ , \qquad (78)$$

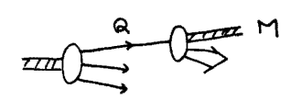

Fig.27.

where $D_Q^M(z)$ is the fragmentation function of a constituent quark Q(p) into a meson(zp)+anything. If we identify $D_Q^M(z)$ with the quark-parton fragmentation function such as $D_q^M(z) \sim z^{-1}(1-z)$, and

use Eq.(77), we obtain the behavior

$$x\frac{dN}{dx} \propto (1-x)^{2A+1}\int_0^1 \frac{dt\ t^{2A-1}(1-t)}{[1-(1-x)t]^{2-A}} \qquad (79)$$

The value A=1 is compatible with the data $(1-x)^3$, while A=2 is excluded. (By the way, if we consider the convolution of quark-parton distribution in the proton and its fragmentation, we obtain $xdN/dx\sim(1-x)^5$, similar to the case A=2, and the absolute normalization too small.[15]) As for the normalization in Eq.(78), we should subtract the possibility that some of the valence constituents go into the leading baryon.

Similarly, we may discuss meson distribution from meson beams, starting from the joint distribution:

$$P^{VV}(x_1,x_2) = \frac{\Gamma(2A)}{\Gamma(A)^2}(x_1x_2)^{A-1}\delta(1-x_1-x_2)\ , \qquad (80)$$

which gives

$$P^{V}(x_1) = \frac{x_1^{A-1}(1-x_1)^{A-1}}{B(A,A)} \qquad (81)$$

Convoluting this with $D_Q^M(z)\sim z^{-1}(1-z)$, we obtain

$$x\frac{dN}{dx} \propto (1-x)^{A+1}\int_0^1 \frac{dt\ t^{A-1}(1-t)}{[1-(1-x)t]^{2-A}} \qquad (82)$$

In order to match with the data, which behaves roughly as $\sim(1-x)^{0\sim1}$, the parameter A should not be as large as 1. Minakata[45] adopted A=1/2, requiring the Regge behavior $P^V(x_1)\sim x_1^{-1/2}$ at $x_1\sim0$.

An extreme possibility A~0, which implies

$$P^{V}(x_1) \sim \frac{\delta(x_1)+\delta(x_1-1)}{2} \qquad (83)$$

was suggested by Lund group,[49] presupposing that the configuration x~1 is biased leaving the other at x~0 so as to interact with the other hadron. They have also studied the role of vector meson production, and obtained the ratio 3:1 for direct vector and pseudoscalar productions in the quark cascade model, and the distribution of direct mesons, $D_q^{d.M}(z)$=const..

Thus, the fragmentation of the constituent quark gives resonable results adjusting the value of A and identifying $D_Q^M(z)$ with the quark parton fragmentation. However, there is no firm reason that the dressed quark fragments in the same way as the naked one does. Actually the K^+/π^+ ratio from u-quark seems to be quite different between them: the data shows $pp\to K^+/\pi^+\sim0.5$ at large $x_T=2p_T/\sqrt{s}$ and 90° which may be due to the u-parton fragmentation,[50] while ~0.1 at large x_q and small angles where dressed u-quark may be dominant.

7. Quark-diquark chain model and dual sheet picture

In the additive quark picture, a baryon is regarded as a simple sum of three constituent quarks, and the effect of confinement is tentatively disregarded. However, there are some indications that, when we devide a baryon into a constituent quark and the rest, the remaining diquark system is more energetic than the shape of the baryon spectra in pp collisions, extending to large x.

Another indication is that the energy loss of the beam like state inside a nucleus in p-nucleus collisions seems to be quite small. Therefore, it may be fruitful to investigate the possibility that a baryon behaves as a quark-diquark system.[51] If we incorporate this picture with the quark chain model discussed in section 3.2, we obtain a simple and unified model of meson, baryon and atibaryon productions from any beam of hadrons.[14] Now we discuss this model and related problems concerning dual topological picture.

7.1. Quark-diquark chain model

Let us assume that mesons, baryons and antibaryons are emitted from the chains of quark and diquark such as illustrated in Fig.28.

This assumption leads to the coupled cascade equation of $\bar{q}$ and qq (q and $\bar{q}\bar{q}$) for i → c+anything where i=$\bar{q}$,qq and c=M,B,$\bar{B}$, as follows:

$$g_i^c(z) = k_i^c(z) + \sum_j \int_z^1 \frac{dx}{x} f_i^j(x)\, g_j^c\left(\frac{z}{x}\right) . \qquad (84)$$

This equation is a generalization of Eq.(28), characterized by basic subprocesses shown in Fig.29.

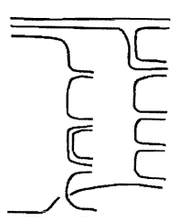

Fig. 28.

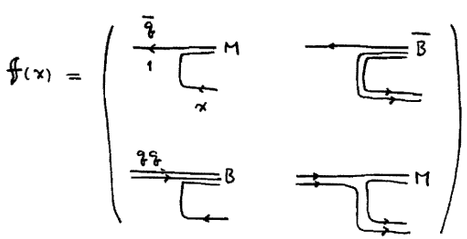

Fig. 29.

Given the function f(x), which determines k(z) by a relation similar to Eq.(29), we may obtain the solution in moment space,

$$\tilde{g}(J) = [1-\tilde{f}(J)]^{-1}\, \tilde{k}(J) . \qquad (85)$$

The hadron distribution from beam hadron a is obtained from the convolution

$$\frac{x dN_a^c}{dx} = \sum_i \int_x^1 \frac{dx_i}{x_i}\, h_a^i(x_i)\, g_i^c\left(\frac{x}{x_i}\right) , \qquad (86)$$

where we put

$$h_M^q(x) = h_M^{\bar{q}}(x) = x P_M^V(x) = \frac{x^A (1-x)^{A-1}}{B(A,A)} , \qquad (87)$$

as Eq.(81) for mesons, while

$$h_B^q(x) = \frac{x^A (1-x)^{\bar{A}-1}}{B(A,\bar{A})} ,$$
$$h_B^{qq}(x) = \frac{x^{\bar{A}} (1-x)^{A-1}}{B(A,\bar{A})} , \qquad (88)$$

for baryons. We may relate the parameters A and $\bar{A}$ to the intercepts of effective M_2 and M_4 meson trajectories (M_2~$q\bar{q}$, M_4~$qq\bar{q}\bar{q}$), as

$$h_M^q(x=\frac{m^2}{s}) \sim s^{-A} \sim s^{\alpha_{M_2}(0)-1} ,$$
$$h_B^{qq}(x=\frac{m^2}{s}) \sim s^{-\bar{A}} \sim s^{\alpha_{M_4}(0)-1} . \qquad (89)$$

(We note that $\alpha(0)$ is defined as the leading pole in moment (J) space.)

Plausible values are $0.5 \lesssim A \lesssim 1$, $1.5 \lesssim \bar{A} \lesssim 2$, corresponding to $0 \lesssim \alpha_{M_2}(0) \lesssim 0.5$ and $-1 \lesssim \alpha_{M_4}(0) \lesssim -0.5$.

As for the emission kernel f(z), we put

$$f_{\bar{q}}^{\bar{q}}(z) = (1-\varepsilon)\frac{z^A(1-z)^{2A-1}}{B(A,2A)}, \qquad f_{\bar{q}}^{qq}(z) = \varepsilon\frac{z^{\bar{A}}(1-z)^{A+\bar{A}-1}}{B(\bar{A},A+\bar{A})},$$
$$f_{qq}^{\bar{q}}(z) = (1-\eta)\frac{z^A(1-z)^{A+\bar{A}-1}}{B(A,A+\bar{A})}, \qquad f_{qq}^{qq}(z) = \eta\frac{z^{\bar{A}}(1-z)^{2A-1}}{B(\bar{A},2A)}, \tag{90}$$

where the exponents of z and 1-z are determined according to the quark and diquark contents of j and c, repectively, in $i \to j+c$. In Eq.(90), we have imposed the normalization condition

$$\sum_j \int_0^1 \frac{dz}{z} f_i^j(z) = 1, \tag{91}$$

which implies the constancy of non-diffractive cross section. Since $B\bar{B}$ pair creations are very small, we can evaluate ε from antibaryon production from meson beam, for example. On the other hand, η is related to the energy dependence of the $p\bar{p}$ annihilation cross section as

$$\sigma(p\bar{p} \to \text{mesons}) \sim s^{(\eta-1)\bar{A}}, \tag{92}$$

since it is determined by the diquark cascade with meson emissions only.

As a compromise of phenomenological survey, we found that

gross feature of meson, baryon and antibaryon distributions from meson and baryon beams can be described by putting[14]

$$A \simeq 0.5, \quad \bar{A} \simeq 2, \quad \varepsilon \simeq 0.15, \quad \eta \simeq 0.25. \tag{93}$$

Aside from details of the model parameters, it is to be stressed that the above scheme gives a unified view of multihadron production in soft, non-diffractive hadron collisions.

7.2. Are quark jets universal ?

Now we discuss the interrelation between jets induced by dressed and naked quarks. For simplicity, we tentatively disregard diquarks, baryons, and QCD hard interaction of $O(\alpha_s)$. According to the quark chain picture, multihadron processes in lepton- and meson-induced reactions are described as shown in Fig.30.[12,52,53]

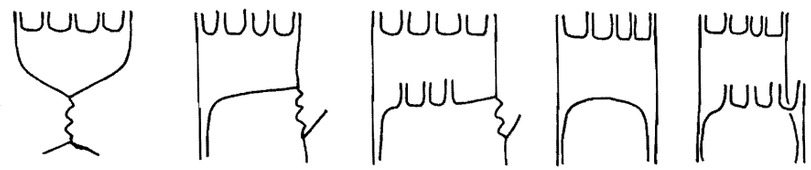

(a) $e\bar{e} \to$ hadrons. (b) Valence term. (c) Sea term. (d) Planar term. (e) Non-planar term.

Fig. 30.[12,52,53]

In the lepton-meson processes, (b) and (c), final state configuration can be regarded as essentially colinear in the C.M.S. of the virtual photon(or W-boson) plus the target meson.

It may be quite tempting to assume the universality of quark chains concerning their dynamical properties. Then, final states in (a), (b) and (d) turn out to be the same (except for the flavor

structure). On the other hand the non-planar term (e) should have hadron density in the central region twice as those in (a), (b) and (d), because of the two-chain structure, while the sea term (c) should have hadronic plateau as (e) and current plateau as (a), with a step in between. This possibility has been supported by majority of people relying on dual sheet picture reinforced by $1/N_c$ expansion argument,[52] or from the fire-sau sage model.[53]

Different possibility should be kept in mind. Although net flavor flows of various processes are as described in Fig.30, dynamical contents behind them may be quite different. I have been insisting on two-types of quark-chains according to dressed or naked quark as the parent.[12] In other words, jets along initial hadron direction and along kicked parton direction in Fig.1 may be quite different, because the former comes from a bunch of partons hopefully described in terms of dressed quark, in contrast to the latter from single parton. If we adopt the dimensional counting for quark-parton→meson+anything, we have $g(z)\sim 1-z$ at $z\sim 1$.[54] On the other hand, we have dressed-quark→meson + anything as $g(z)\sim (1-z)^{A-1}$ with $A\sim 0.5$, different from the above.

Thus, in order to extract definite conclusion, much more studies are necessary.

8. Space-time evolution of production processes

For the through understanding of the dynamics of multihadron production, it is very important to investigate the space-time evolution of production processes, both theoretically and

experimentally. Of course, in high energy experiments we are only looding at the final states after a time scale quite longer than that characteristic to strong interaction, $\sim 10^{-23}$ sec. Fortunatelly, the usage of nucleus targets provides a mean to look into the evolution of the processes by changing the size of the nucleus, as I will discuss in the next section. In this section I will briefly review theoretical arguments on space-time evolution.

8.1. Realistic quark cascade

As a basis of the cascade relation (28), Fukuda and Iso[9] assumed a diffusion equation for the cascading quark density $Q(z,t)$ in dz at time t as

$$\frac{\partial Q(z,t)}{\partial t} = -(\lambda+\lambda')Q(z,t) + \lambda\int_z^1 \frac{dz'}{z'} F(\frac{z}{z'})Q(z',t) \ , \qquad (94)$$

where λ is the emission probability for $q \to q'$+Meson per unit time. With the normalization

$$\int_0^1 dz F(z) = 1 \ , \qquad (95)$$

$\lambda'$is regarded as the absorption probability per unit time. Actually, in the proton beam jet, the absorption is due to the recombination with other cascading quarks to form a baryon, while $\lambda'=0$ for the quark jet in the e^+e^- annihilation.

The time dependence of the meson distribution is given by

$$\frac{\partial M(x,t)}{\partial t} = \int_x^1 \frac{dz}{z} Q(z,t)\lambda F(1-\frac{x}{z}) \ . \qquad (96)$$

With the initial condition $Q(z,t=0)=\delta(1-z)$ and $M(x,t=0)=0$, we obtain the distribution at $t=\infty$ as follows:

$$M(x) \equiv M(x,t=\infty) = \int_x^1 \frac{dz}{z} Q(z)\lambda F(1-\frac{x}{z}) \ , \qquad (97)$$

where

$$Q(z) = \int_0^\infty dt Q(z,t) \ . \qquad (98)$$

Since $Q(z,t=\infty)=0$ for $z>0$, we obtain the following equation by integrating Eq.(94):

$$Q(z) = \frac{1}{\lambda+\lambda'}\delta(1-z) + \frac{\lambda}{\lambda+\lambda'}\int_z^1 \frac{dz'}{z'} F(\frac{z}{z'})Q(z') \ .$$

Substituting this into Eq.(97), we have

$$M(x) = \alpha\cdot F(1-x)+\int_x^1 \frac{dz}{z}\int_z^1 \frac{dz'}{z'}\alpha F(\frac{z}{z'}) \ Q(z') \ \lambda F(\frac{z-x}{z}) \ . \qquad (99)$$

where $\alpha=\lambda/(\lambda+\lambda')$. We rewrite the second term in Eq.(99) as

$$\int_x^1\frac{dz}{z}\int_0^1 dz'\int_0^1 dX\,\delta(z-Xz')\alpha F(X)Q(z')\lambda F(1-\frac{x}{z})$$
$$=\int_x^1 \frac{dX}{X}\,\alpha F(X)\int_{\frac{x}{X}}^1 \frac{dz'}{z'} \ Q(z') \ \lambda F(1-\frac{x/X}{z'})$$
$$=\int_x^1 \frac{dX}{X}\,\alpha F(X)M(\frac{x}{X}) \ .$$

Thus, we have

$$M(x) = \alpha F(1-x) + \alpha\int_x^1 \frac{dX}{X} F(X)M(\frac{x}{X}) \ . \qquad (100)$$

For $\alpha=1$, the above equation reduces to Eq.(28), where $g(x)=xM(x)$ and $f(x)=xF(x)$.

If we take into account the time dilation as Sawada,[10] Eqs.(94) and (96) are to be slightly modified as

$$\frac{\partial Q(z,t)}{\partial t} = -\frac{\lambda+\lambda'}{z} Q(z,t) + \int_z^1 \frac{dz'}{z'} F(\frac{z}{z'})\frac{\lambda}{z'} \ Q(z',t) \ , \qquad (101)$$

$$\frac{\partial M(x,t)}{\partial t} = \int_x^1 \frac{dz}{z} \ Q(z,t)\frac{\lambda}{z} \ F(1-\frac{x}{z}) \ , \qquad (102)$$

where the emission and absorption probabilities are denoted as λ and λ' at $z=1$, respectively, and they increase into λ/z and λ'/z at $z<1$. However, the final result of $M(x)=M(x,t=\infty)$ is the same as before.

8.2. Inward-outward cascade

In the diffusion equation we have just discussed, the space time evolution of the hadronization proceeds as follows: an initial fast moving quark radiates mesons and gradually slows down to $z=0$, occationally recombines with others for $\lambda'=0$. Therefore, relatively fast mesons are produced at stages earlier than slow mesons. This type of evolution is similar to successive decays of massive resonance and to the bremstrahlung process of high energy particle in a medium.

However, as we have stressed in sect. 3.2, the hadronization of a quark jet is not an isolated decay process but the result of final state confinement interaction. Along this line of thought, we may take the picture that the hadronization is the color

neutralization process of $q\bar{q}$-pair creations through the vacuum polarization by color flux and the recombinations of neighboring q and $\bar{q}'$ into colorless clusters which are hadrons or excited states. Then, it seems more reasonable that the creations of colorless clusters are independent of each other, occurring at relatively spacelike positions. Therefore, in the case of $e^+e^- \to q\bar{q} \to$ hadrons, the space-time evolution in the C.M.S. may be illustrated as Fig.31, where slow hadrons are produced first, and fast hadrons later. This type of evolution is named "inward-outward cascade" by Bjorken,[55] in contrast to the "outward-inward cascade" shown in Fig.32, which is often implicitly assumed in fragmentation models. However, the face result of the diffusion equation may be described as Fig.33, where slowed down q and $\bar{q}$ become widely separated each other.

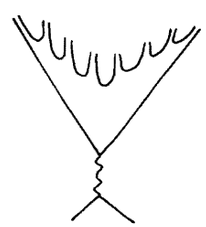

Fig.31.

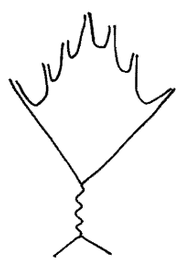

Fig.32.

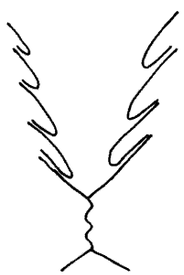

Fig.33.

Recently, a model of inward-outward cascade was presented by Toriu on the basis of string picture for the stretching $q\bar{q}$ state before the hadronization.[56] He assumed that the hadronization takes place on a spacelike hypersurface characterized by a "life time" of the stretching string, as a break up into many short strings with uniform possibility of breaking per unit length of

initial string. Regarding the short strings as final mesons, he obtained the same meson distribution $g(x) \sim \lambda(1-x)^{\lambda-1}$ as due to the cascade relation with $f(z)=\lambda z^{\lambda}$. However, this nice result rests on the situation that a meson with large x should have large mass, which is determined by the length of the string.

The cascade relation was also derived by Lund group[57] assuming pair creation of $q\bar{q}$ with uniform probability per unit length in a constant field in the (1+1)-dimension at arbitrary time. Although this is a semi-classical model and existence of hadrons with discrete masses should be put in by hand, it may be regarded as a very natural realization of the inward-outward cascade by the confinement force.

8.3. Multiperipheral parton model

In order to understand the evolution of multiparticle processes in hadron-hadron and hadron-nucleus collisions, Koplik and Mueller examined the time development of the multiperipheral diagram in the scalar ϕ^3 theory.[58] In the laboratory frame, the process is described as Fig.34, where the incoming hadron starts to dissociate before reaching a target and extends a multiperipheral arm down to the wee region, $y_{Lab} \sim 0$, so as to be able to interact with the target. This is the multiperipheral parton picture and in accordance with the assumption of the short distance interaction in rapidity. However, it is not clear when and where final state hadrons are produced, since the difference between hadrons and constituents is not recongnized in this model. If we regard that the products from the arm are partons, we may take the picture that the recombination of them occurs at a spacelike surface after

the collision, described by the dotted line in Fig.35. Then, in the laboratory frame, the slow particles are produced first, as in the inward-outward cascade.

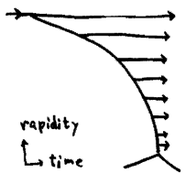

Fig. 34.

Fig. 35.

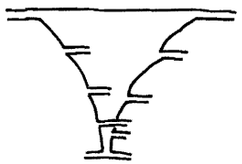

Fig. 36.

Another possibility may be to regard the ϕ^3 interaction as the dissociation vertex of a meson into q and $\bar{q}$, and take the picture shown in Fig.36.

It should also be mentioned that there are QCD motivated models which are against the hypothesis of short rapidity distance interaction which presumed the softness of strong interaction. Low and Nussinov adopted one gluon exchange between valence quarks in the beam and the target as a dominant mechanism giving constant cross section.[59] This mechanism leads to the multihadron production as the result of color neutralization process. Brodsky and Gunion considered the exchange of a wee quark between the beam and the target, so as to cause the triplet color separation as a pre-stage of multihadron production.[60]

In spite of such efforts as above, theoretical understanding of the time evolution of hadronic multiparticle processes is still in its infancy, because it is intimately related with the problems of

composite hadron structure and confinement. Therefore, at the present status, it may be fruitful to develop phenomenological models in close contact with the data on nucleus targets.

9. Nucleus target as the apparatus to measure jet evolution

The nucleus target is an essetial tool to study jet evolutions during microscopic time and distance, both in lepton- and hadron-induced reactions. Deep inelastic lepton scattering on the nucleon inside a nucleus provides tagged quark-parton beam for quark-nucleon interaction, and the oppotunity to test the hypothesis of inward-outward cascade discussed in Sect.8.2, by studying how the kicked out quark traverses the nucleus and eventually turns into a jet of hadrons before or after coming out of it. Thus fascinating, however, experimental studies are still preliminary[61] and phenomenological analysis seems to require much devotion.[62]

On the other hand, there are accumulated data and analyses concerning hadron-nucleus reactions. In the following, I will discuss particle distributions in soft hadron-nucleus collisions.

9.1. Characteristic features of the data

We may summarize the prominent features of the data on hadron-nucleus reactions at small p_T as follows:[63]

(A) The mean multiplicity depends only mildly on the mass number A of the nucleus. In terms of "mean collision number"

$$\bar{\nu} \equiv \frac{A\sigma_{inel}^{hN}}{\sigma_{inel}^{hA}} , \qquad (103)$$

it is described by

$$\langle n \rangle_{hA} \simeq \frac{1+\bar{\nu}}{2} \langle n \rangle_{hN} . \qquad (104)$$

This excludes the naive intra-nuclear cascade in which all of the produced particles at each step of the collision with a nucleon inside the nucleus undergo secondary interactions with other nucleons downstream in the nucleus as ordinary hadron-nucleon interactions, since this model gives too strong dependence of $\langle n \rangle_{hA}$ on A.

(B) The single-particle distribution in pseudorapidity,

$$\eta = -\ln[\tan \frac{\theta_{Lab}}{2}] ,$$

which is approximately regarded as the rapidity $y=\frac{1}{2}\ln(p_+/p_-)$ in the laboratory system, shows overall increase in the central and target fragmentation regions. The ratio

$$R_{hA}(\eta) \equiv \frac{dN^{hA}}{d\eta} / \frac{dN^{hA}}{d\eta} \qquad (105)$$

behaves as

$$R_{hA}(\eta) \sim \bar{\nu} \quad \text{in the central region,}$$
$$\lesssim 1 \quad \text{in the beam frag. region.}$$

This behavior indicates independent collisions with $\bar{\nu}$ nucleons in the nucleus. The behavior in the beam fragmentation region is constrained by overall energy momentum conservation.

(B') In the target fragmentation region, $\eta \lesssim 1$, it is observed that

$$R_{hA}(\eta) > \bar{\nu} .$$

This trend is stronger for lower η. Furthermore, anomalous backward production is observed beyond the kinematical boundary of independent hN collision.

(C) For different beams (π^+, K^+, p) and nuclei, the universality $R_{hA}(\eta)=R_{\bar{\nu}}(\eta)$ is satisfied with remarkable accuracy, indicating $\bar{\nu}$ to be an excellent scaling parameter.

(D) The Glauber-Gribov type multiple scattering theory works very well for the A and beam dependences of inelastic cross section σ_{inel}^{hA} within 10%. Therefore, $\bar{\nu}$ can be regarded as the effective thickness of the nucleus.

(E) The leading nucleon distributions from the nucleon beams depend on A only weakly, exhibiting that the energy loss of the beam-like state is rather small, different from $NN \to NX$.

Furthermore, there are interesting data on nuclear targets concerning large p_T hadron production, which are not covered here.

9.2. Multi-chain model

Various models have been proposed to explain some of the data, based on field theoretical arguments, composite structure of hadrons, and/or empirical assumptions.[64] Fortunately, the prominent

features of the data listed in 9.1, taken altogether, are already very restrictive for possible mechanisms. Namely, almost unique picture compatible with all of (A)∼(E) is that the beam-like state collides successively with nucleons traversing the nucleus, producing particles at each collision as in ordinary hadron-nucleon collisions, where produced particles comes out almost without secondary interaction, as illustrated in Fig.37. This picture is formulated as the multi-chain model of sequential collision type.[65] In the following, I will briefly recapiturate this model.

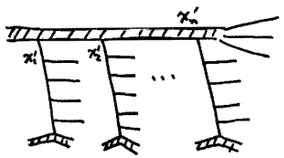

Fig.37. Multi-chain model of sequential collision type.

We put the charged particle distribution in h-A collision as

$$\left(\frac{dN}{dy}\right)_{hA} = \sum_{n=1}^{A} W_{\bar{\nu}}(n) \sum_{i=1}^{n} \int_{x}^{1} dx_i' \, \tilde{F}_n^i(x_i') \, G\left(\frac{x}{x_i'}, x_-\right) , \qquad (106)$$

where $W_{\bar{\nu}}(n)$ is the probability that n-collision process takes place inside the nucleus specified by $\bar{\nu}$, $\tilde{F}_n(x_i')$ is the probability density that the i-th chain in the n-collision process has the momentum fraction x_i' of the incoming hadron, $G(x_+,x_-)$ is defined by

$$\left(\frac{dN}{dy}\right)_{hN} = G(x_+,x_-) , \qquad x_- = \frac{E-p_\parallel}{m_N} , \qquad (107)$$

in the laboratory frame, and $x=(E+p_\parallel)/(E+P)_{beam}$. In order to

accomodate the dissociation of the beam -like state at the final step, we identify x_n' for the last chain as indicated in Fig.37, for simplicity. We have seen that Eq.(106) reproduces the data with wide choices $\tilde{F}_n^i(x_i')$, even including average equipartition $\langle x_i' \rangle = 1/n$.[66] If we further require the property (E) for the leading nucleon spectra, we may single out the sequential collision type with small energy loss (∼15%). The only defect of this model is $R_{\bar{\nu}}(n) \simeq \bar{\nu}$ in the target fragmentation region, not in accord with (B'), which can be partly remedied by considering the secondary interaction of recoil nucleons.[67]

It may be interesting to infer the above model from quark-gluon dynamics. The absence of the secondary interaction of produced particles, except for recoil nucleon or slow particles, indicates that the hadronization time is long enough, or the nucleus is almost transparent against newly born particles regarded as seeds of hadrons. In other words, it takes time for them to grow up to ordinary matured hadrons with enough glue. On the other hand, the beam-like state can interact with nucleons repeatedly in a way similar to the beam-nucleon collision, without much wounded at each step. This is in contrast to the additive quark model with inelasticity ∼1.0 for the quark-nucleon interaction.[68] The energy loss in the q-N interaction may be rather small in the additive picture, or the interacting quark is already slow in the quark-diquark picture. Anyhow it is very important to clarify theoretical basis for sucessful picture of hadron-nucleus interaction.

10. Concluding remarks

We have discussed various approaches to the dynamics governing the formation of jets of hadrons. Although different models do not converge into one goal so quickly, we may still extract some general instructions. In the following, I try to summarize them without suppressing my prejudice, and add a few remarks.

(1) Physics in terms of the momentum fraction $x_\pm$ or z, rapidity y and moment n or J ("angular momentum" conjugate to y) are mutually permutable. Therefore, central and fragmentation dynamics can be treated on the same footing.

(2) The $(1-x)^n$ behavior at large x comes out in various models owing to the energy momentum conservation. Furthermore, the beta distribution $x^m(1-x)^n$ is a useful expression to discuss data and models, where exponents m and n reflect the essence of underlying dynamics.

(3) The memory of initial quark, irrespective to dressed or naked, is preserved in a fast hadron containing it, seen from the flavor structure of hadron distribution. At small p_T, this is realized in different ways, i.e., recombination and fragmentation (including cascade and chain) models.

(4) The perturbative QCD approach provides jet shower of partons up to pre-confinement stage, which is expected to continue smoothly to non-perturbative, confinement stage of hadronization.

(5) The quark-chain structure incorporating the cascade relation seems to embody essential features of hadronic final states in various reactions. This picture provides a unified understanding

of iclusive distributions and exclusive multiparticle distributions.

(6) The understanding of hadronization process on the basis of non-perturbative confinement dynamics is remaining as an open and challenging problem. The quark-chain model may be regarded as an intermediate goal to reach from theoretical side. There, the question is remaining : Are quark jets universal ?

(7) Incorporation of baryons into the quark chain is easily done by treating the diquark as the additional link element of the chain. It is not yet clear whether it is deeply rooted on quark-diquark structure of baryons, or compatible also with some other model of baryon structure.

(8) Multiparticle production on nucleus targets provides peculiar informations on the space-time evolution of the hadronization process. The hadron beam data are already restrictive enough to single out the multi-chain model of sequential collision type as the most successful one. Theoretical understanding of the mechanism embodied in this model is remaining as very interesting problem.

(9) The frontiers of the jet dynamics are widely open. Precise data of two-hadron distributions at Fermilab energies started to come out very recently. Furthermore, there are new types of experiments not much explored. Some of them are gluon jets, heavy quark jets, associated hadrons with lepton-pair productions, lepton-nucleus reactions, and so on. Let us look forward to make great advances in 1980's by working hard together experimentally, phenomenologically and theoretically.

I wish to thank the Organizing Committee of the KEK Summer School (National Laboratory for High Energy Physics), and

Prof. K.Niu (Nagoya) for invited me to have the oppotunities to summarize the jet dynamics. I am also grateful to Prof. S.Kagiyama for valuable discussions and careful reading of the manuscript, and to Mis S.Wada for her devotion and perseverence in typing within limited term.

References

1) Forward and backward jets : G.Giacomelli, Tokyo Conf. (Proc. 19th Int. Conf. H.E.Phys., Tokyo 1978), p.53; J.Whitemore, ibid., p.63, for reviews.
The e^+e^- jets : G.G.Hanson et al., Phys. Rev. Lett. 35 (1975), 1609.
Jets in lepton-hadron reactions : D.R.O.Morrison, IX Multiparticle Symposium, Tabor, Fl, for a review.

2) M.Jacob and P.V.Landshoff, Phys. Rep. 48C (1978), 286, for a review.

3) W.Marciano and H.Pagels, Phys, Rep. 36C (1978), 137, for a review.

4) F.Halzen, Tokyo Conf. (1973), p.214; R.D.Field, ibid., p.743 for reviews.

5) PLUTO Cllab., Phys. Lett. 82B (1979), 449.
DHHMM Collab., Phys. Lett. 86B (1979), 399.

6) D.P.Barber et al., Phys. Rev. Lett. 43 (1979), 830.
PLUTO Collab., Phys. Lett. 86B (1979), 418.

7) R.P.Feynman, Photon-Hadron Interactions, Benjamin (N.Y.), 1972.

8) Yu.L.Dokshitser and K.-I.Dyakonov, DESY L-Trans-24 (1979), for a review.

9) H.Fukuda and C.Iso, Prog. Theor. Phys. 57 (1977), 483, 1663; Hakone Workshop (Proc. Multiparticle Dynamics, Hakone,Sept. 1978), p.244, and references therein.

10) O.Sawada, Prog. Theor. Phys. 58 (1977), 1815.

11) R.D.Field and R.P.Feynman, Nucl. Phys. B136 (1978), 1.

12) K.Kinoshita, Nuovo. Cim. 34A (1976), 413; Kazimierz Symposium (Proc. I Int. Sympl on Hadron Structure and Multiparticle Production, Kazimierz,May 1977), p.355.

13) T.Kawabe, Y.Ohtani and K.Kinoshita, Z. Physik C2 (1979), in press.

14) K.Kinoshita, H.Noda, T.Tashiro and M.Mizouchi, Z. Physik C3 (1980), in press.

15) K.P.Das and R.C.Hwa, Phys. Lett. 68B (1977), 459.
D.W.Duke and F.E.Taylor, Phys. Rev. D17 (1978), 1788.
R.C.Hwa and R.G.Roberts, Z.Physik C1 (1979), 81.

16) L.Van Hove and S.Pokorski, Nucl. Phys. B86 (1975), 243.

17) T.Kanki, Prog. Theor. Phys. 56 (1976), 1885; ibid. 57 (1977), 1641.
T.Kanki, Y.Okamoto and S.Ryang, ibid. 58 (1977), 1830.

18) B.Andersson, G.Gustafson and C.Peterson, Phys. Lett. 69B (1977), 221; ibid. 71B (1977), 337; Nucl. Phys. B135 (1978), 273.

19) K.Kinoshita and H.Noda, Prog. Theor, Phys. 47 (1972), 1300; Int. Symp. on H. E. Physics, Tokyo, 1973, p.403.
D.Currs et al., Phys. Rev. Lett. 43 (1979), 319 for recent data.

20) L.Van Hove, Nuovo Cim. 28 (1963), 798.
A.Krzywicki, Nuovo Cim. 32 (1964), 1069.
21) E.H. de Groot, Nucl. Phys. B48 (1972) 295.
R.Baier et al., Nuovo Cim, 28A (1975) 455.
22) J.Kuti and W.F.Weisskopf, Phys. Rev. D4 (1971), 3418.
23) e.g., F.E.Close, CERN TH.2594 (1978) and references therein.
24) R.McElhaney and S.F.Tuan, Phys. Rev. D8 (1973), 2267.
C.B.Chiu et al., Phys. Rev. D20 (1979), 211.
25) A.Casher, J.Kogut and L.Susskind, Phys. Rev. D10 (1974), 732.
26) G.Veneziano, Nucl. Phys. B117 (1976), 517; Tokyo Conf. (1978), p.725.
A related approach by Y.Igarashi, T.Matsuoka and S.Sawada, Prog. Theor. Phys. 57 (1977), 499; T.Matsuoka, Hakone workshop (1978), p.61. T.Kitazoe and T.Morii, preprints KULA-HE-79-1,5,6(1979).
27) Y.Fujimoto et al. (Japan-Brasil coll.), Prog. Theor. Phys. Suppl. 47 (1971),1; ibid. 54 (1973),1; Hakone Workshop (1978), p.22.
M.Hama and M.Nagasaki, Hakone Workshop (1978), p.47 and references therein.
S.Kagiyama, Prog. Theor. Phys. 54 (1975). 166.
J.Ranft, Vth Multiparticle Symposium, Leipzig 1974, p.210 for a review.
28) H.Noda and T.Tashiro, Prog. Theor. Phys.62 (1979), No.4.
29) J.Kogut and L.Susskind, Phys. Rev. D9 (1974), 697, 3391.
T.Uematsu, Prog. Theor. Phys.56 (1976), 1599.
30) G.Altrarelli and G.Parisi, Nucl. Phys. B126 (1977), 298.
31) K.Konishi, A.Ukawa and G.Veneziano, Phys. Lett. 78B (1978), 243; ibid. 80B (1978), 259. preprint RL 79-026 (1979).

32) D.Amati and G.Veneziano, Phys. Lett. 83B (1979), 87.
A.Bassetto, M.Ciafaloni and G.Marchesini, Phys. Lett. 83B (1979), 207; preprint SNS 4/1979.
33) G.Sterman and S.Weinberg, Phys. Rev. Lett. 39 (1977), 1436.
34) W.Ochs, Nucl. Phys. B118 (1977), 397.
H.Goldberg, Nucl. Phys. B44 (1972), 149.
35) T.A.De Grand and H.I.Miettinen, Phys. Rev. Lett. 40 (1978), 612.
36) C.B.Chiu et al., loc. cit. 24).
37) M.Biyajima and O.Miyamura, Prog. Theor. Phys. 51 (1974), 1455.
N.Nakamaru, Doctor Thesis, Tokyo Univ. of Education (1974).
38) K.Böckmann, I Kazimerz Symposium (1977), p.21.
S.Nandi, V.Rittenberg and H.R.Schneider, Phys. Rev. D17 (1978), 1336.
39) K.Kinoshita and H.Noda, Prog. Theor. Phys. 50 (1973), 915.
40) J.Kalinowski, S.Pokorski and L.Van Hove, Z. Physik C2 (1979), 85.
41) J.Ranft, Phys. Rev. D18 (1978), 1491.
42) M.G.Albrow et al. (BSF-Collab.), Nucl. Phys. B135 (1978), 461.
43) H.Satz, Phys. Rev. Lett. 19 (1967), 1453; Phys. Lett. 25B (1967); 220; Invited Talk at Budapest Conf., 1977.
44) V.V.Anisowich and V.M.Shechter, Nucl. Phys. B55 (1973), 455.
45) H.Minakata, Phys. Rev. D, in press (preprint TMU-HEL-902, 1979).
K.Hagiwara and K.Kanai, preprint TMUP-HEL-806 (1978).
H.Senju, Prog. Theor. Phys. 58 (1977), 1651; ibid. 59 (1978),868.
46) G.Altarelli et al., Nucl. Phys. 69B (1974), 531.
47) K.Hirose and T.Kanki, preprints OS-GE 78-17 (1978), 79-20,21 (1979).
48) M.Glück and E.Reya, Nucl. Phys. B130 (1977), 76.

N.Cabibbo and R.Petronzio, Nucl. Phys. B137 (1978), 395.

49) B.Andersson, G.Gustafson and C.Peterson, loc. cit. 18).

50) D.Antreasyan et al., Phys. Rev. Lett. 38 (1977), 112, 115.

51) e.g. G.F.Chew and C.Rosenzweig, Nucl. Phys. B117 (1976),519.
S.Ono, Aachen preprint (1979).

52) G.Veneziano, Nucl. Phys. B117 (1976), 519.
J.Dias de Deus and S.Jadach, Acta Phys. Pol. B9 (1978), 249.
H.Minakata, loc. cit. 45).
A. Capella et al., Phys. Lett. 81B (1979), 68.

53) N.S.Craigie and G.Preparata, Nucl. Phys. B102 (1976), 497.

54) S.Brodsky and G.Farrar, Phys. Rev. Lett. 31 (1973), 1153;
Phys. Rev. D11 (1975), 1304.

55) J.D.Bjorken, Summer Inst. of Particle Physics, SLAC-167 (1973).

56) Toriu, Prog. Theor. Phys. 61 (1979), 218.
See also X. Artru and G.Mennessier, Nucl. Phys. B70 (1974), 93.

57) B.Andersson, G.Gustafson and C.Peterson, Z. Physik C1 (1979), 105.

58) J.Koplik and A.H.Mueller, Phys. Rev. D12 (1975), 3638.
See also J.Kogut and L.Susskind, Phys. Rep. 8C (1973), 76.

59) F.Low, Phys. Rev. D12 (1975), 163.
S.Nussinov, Phys. Rev. Lett. 34 (1973), 1286.

60) S.J.Brodsky and J.F.Gunion, Phys. Rev. Lett. 37 (1976), 402;
VII Multiparticle Symposium, Tutzing (1976), p.369.

61) L.S.Osborne et al., Phys. Rev. Lett. 40 (1978), 1624.
L.Hand et al., Acta Phys. Pol. B9 (1978), 1987.
H.C.Ballagh et al., Phys. Lett. 79B (1978), 320.

62) S.Brodsky et al., Phys. Rev. Lett. 39 (1977), 1120.
G.V.Davidenko and N.N.Nikolaev, Nucl. Phys. B135 (1978), 333.

63) For reviews, C.Halliwell, VIII Multiparticle Symposium,
Kaysersberg, (1977), p.D-1; T.Ferbel, Tokyo Conf. (1978), p.465.

64) For reviews, B.Andersson, VII Multiparticle Symposium, Tutzing,
(1976), p.109; A.Białas, IX Multiparticle Symposium, Tabor,
(1978), p.C1.

65) K.Kinoshita, A.Minaka and H.Sumiyoshi, preprint KYSHU-79-HE-5/
KAGOSHIMA-HE-79-5 (1979).

66) A.Capella and A.Krzywicki, Phys. Lett. 67B (1977), 84.
K.Kinoshita, A.Minaka and H.Sumiyoshi, Prog. Theor. Phys. 61
(1979), 165.

67) K.Kinoshita, A.Minaka and H.Sumiyoshi, preprint KYUSHU-79-HE-10/
KAGOSHIMA-HE-79-6 (1979).
For additional or alternative effects, F.Takagi, Prog. Theor.
Phys. 62 (1979), 457.
N.N.Nikolaev et al., loc. cit. 68).

68) A.Białas et al., Acta Phys. Pol. B8 (1977), 585.
N.N.Nikolaev, A.Ya Ostapchuk and V.R.Zoller, CERN preprint
Th.2521 (1978).
V.V.Anisovich, Yu.M.Shabelsky and V.M.Shekhter, Nucl. Phys. B133
(1978), 477.